Differential spatial and temporal phosphorylation of the visual receptor, rhodopsin, at two primary phosphorylation sites in mice exposed to light

Ryan A. ADAMS*, Xinran LIU†‡, David S. WILLIAMS† and Alexandra C. NEWTON†[1]

*Department of Chemistry and Biochemistry, University of California at San Diego, 9500 Gilman Drive, La Jolla, CA 92093-0640, U.S.A., †Department of Pharmacology, University of California at San Diego, 9500 Gilman Drive, La Jolla, CA 92093-0640, USA, and ‡Center for Basic Neuroscience, University of Texas Southwestern Medical Center, 5323 Harry Hines Boulevard, Dallas, TX 75390-9111, U.S.A.

Phosphorylation of rhodopsin critically controls the visual transduction cascade by uncoupling it from the G-protein transducin. The kinase primarily responsible for this phosphorylation is rhodopsin kinase, a substrate-regulated kinase that phosphorylates light-activated rhodopsin. Protein kinase C has been implicated in controlling the phosphorylation of both light-activated and dark-adapted rhodopsin. Two of the major rhodopsin phosphorylation sites *in vivo*, Ser^{334} and Ser^{338}, are effective protein kinase C phosphorylation sites *in vitro*, while the latter is preferentially phosphorylated by rhodopsin kinase *in vitro*. Using phosphospecific antibodies against each of these two sites, we show that both sites are under differential spatial and temporal regulation. Exposure of mice to light results in rapid phosphorylation of Ser^{338} that is evenly distributed along the rod outer segment. Phosphorylation of Ser^{334} is considerably slower, begins at the base of the rod outer segment, and spreads to the top of the photoreceptor over time. In addition, we show that phosphorylation of both sites is abolished in rhodopsin kinase$^{-/-}$ mice, revealing an absolute requirement for rhodopsin kinase to phosphorylate rhodopsin. This requirement may reflect the need for priming phosphorylations at rhodopsin kinase sites allowing for subsequent phosphorylation by protein kinase C at Ser^{334}. In this regard, treatment of mouse retinas with phorbol esters results in a 4-fold increase in phosphorylation on Ser^{334}, with no significant effect on the phosphorylation of Ser^{338}. Our results are consistent with light triggering rapid priming phosphorylations of rhodopsin by rhodopsin kinase, followed by a slower phosphorylation on Ser^{334}, which is regulated by protein kinase C.

Key words: phosphorylation, phototransduction, protein kinase C (PKC), rhodopsin, rhodopsin kinase (RK), signal transduction.

INTRODUCTION

The visual receptor, rhodopsin, initiates phototransduction by its light-dependent coupling to the G-protein, transducin [1–3]. Subsequent deactivation is initiated by phosphorylation of the C-terminus of rhodopsin, an event that promotes arrestin binding and effectively uncouples rhodopsin from transducin. Understanding the molecular mechanisms governing the phosphorylation of rhodopsin is critical to understanding phototransduction.

Extensive studies over the past two decades have firmly established that the G-protein-receptor kinase, rhodopsin kinase (RK), is a central player in rhodopsin phosphorylation [4–9]. This kinase phosphorylates the light-activated conformation of rhodopsin at multiple sites *in vitro*, with its preferred sites being Ser^{338} and Ser^{343} [10,11]. It has also been suggested that a separate kinase, the lipid second-messenger-regulated kinase, protein kinase C (PKC), modulates the phosphorylation of rhodopsin [12]. Treatment of intact retinas with PKC activators (phorbol esters) or inhibitors (calphostin C) alters the light-dependent phosphorylation of rhodopsin [13–15]. This modulation probably reflects direct phosphorylation of rhodopsin by PKC, as studies with pure proteins have revealed that PKC phosphorylates rhodopsin stoichiometrically [16]. This phosphorylation occurs at two C-terminal sites: an RK site, Ser^{338}, and a novel site, Ser^{334} [17].

Important progress into understanding the mechanism of rhodopsin phosphorylation resulted from the finding that the three major *in vitro* sites, Ser^{334}, Ser^{338} and Ser^{343}, are also the sites phosphorylated following exposure of mice to light. Initial MS studies identified Ser^{338} and Ser^{334} as the primary sites that are phosphorylated in live mice exposed to constant light [18]. More recent studies, using novel rapid-quench/MS-based analyses, revealed that a third site, Ser^{343}, also becomes significantly phosphorylated [19]. Functional analyses of rods from transgenic mice expressing rhodopsin mutated in one or more phosphorylation sites reveals that phosphorylation of each site is involved in rhodopsin deactivation, and, specifically, mutation of any of these sites to alanine slows the deactivation kinetics of rhodopsin [20]. The requirement for multiple phosphorylation events to regulate rhodopsin begs the question as to what mechanisms regulate these phosphorylations: are the events ordered, are they catalysed by different kinases, and what is their spatial and temporal resolution?

In the present study, we generated phosphospecific antibodies to address the regulation of rhodopsin phosphorylation at Ser^{334} and Ser^{338}. Our results suggest an ordered phosphorylation of rhodopsin that depends on RK for the first step and PKC for the second step.

EXPERIMENTAL

Materials

Frozen bovine retinas were kindly provided by Dr Yee-Kin Ho (Department of Biochemistry and Molecular Biology, University of Illinois, College of Medicine, Chicago, IL, U.S.A.). Balb/c

Abbreviations used: Ac, acetyl; DMEM, Dulbecco's modified Eagle's medium; EM, electron microscopy; KLH, keyhole limpet haemocyanin; PKC, protein kinase C; pS, phosphoserine; RK, rhodopsin kinase; ROS, rod outer segment.

[1] To whom correspondence should be addressed (e-mail anewton@ucsd.edu).

mice were purchased from Taconic (Germantown, NY, U.S.A.). Nitrocellulose was purchased from Bio-Rad, calf intestinal phosphatase was from New England Biolabs, and PVDF was from Millipore. DMEM (Dulbecco's modified Eagle's medium) was obtained from BioWhittaker. PMA and BSA were purchased from Calbiochem. DMSO was purchased from Sigma. All other chemicals were reagent-grade.

Generation of phosphospecific antibodies

Synthesis of phosphorylated peptides, immunization of rabbits, and collection of sera were performed by Multiple Peptide Systems (San Diego, CA, U.S.A.). The sequence for the peptide containing phosphorylated Ser^{334} was Ac-CLGDDEA-pS-ATAS-NH_2 (where Ac is acetyl), that for the peptide containing phosphorylated Ser^{338} was Ac-CASATA-pS-KTETSQ-NH_2, and that for the peptide phosphorylated at both Ser^{334} and Ser^{338} was Ac-CLGDDEA-pS-ATA-pS-KTETSQA-NH_2, where pS denotes phosphoserine. Mono- and di-phosphorylated peptides were conjugated through the N-terminal cysteine thiol to keyhole limpet haemocyanin (KLH). Monophosphorylated antigens were subcutaneously injected into six New Zealand white rabbits, aged 3–9 months. Antisera from all six rabbits produced phosphospecific antibodies of comparable titre; antibodies from the fourth bleed were affinity purified by applying crude antisera to a gel cross-linked with the appropriate synthetic phosphopeptide. Antibodies were eluted at low pH into a neutralizing buffer. Antibodies are referred to as α-P334 and α-P338; similar results were obtained using crude or affinity-purified antibodies.

Dot blot analysis

KLH and conjugated phosphorylated peptides were spotted at the indicated concentrations on to nitrocellulose in a Schleicher and Schuell vacuum manifold (Keene, NH, U.S.A.). Individual wells were washed with water before removal from the manifold and blocked with 5 % (w/v) non-fat dried milk. Blots were probed with affinity-purified antibody at 1 : 5000 dilution in 1 % (w/v) BSA in PBS-T [PBS with 0.5 % (v/v) Tween 20 and 0.1 % (v/v) thimerosal] solution.

Rhodopsin purification

Rod outer segments (ROSs) were isolated from 50 bovine retinas as described by Papermaster and Dreyer [21]; isolation was performed in the light so that rhodopsin was phosphorylated. Membranes were urea-stripped as described in [16]. ROS membranes were incubated with calf intestinal phosphatase for 20 min at 30 °C to dephosphorylate rhodopsin. Samples were subjected to SDS/PAGE, transferred on to PVDF, and blotted with antisera at 1 : 1000 dilution. Total opsin was detected with the monoclonal 1D4 antibody, kindly provided by Dr Robert Molday (Department of Biochemistry and Molecular Biology, University of British Columbia, Vancouver, BC, Canada).

In vitro rhodopsin phosphorylation

Dark-adapted, urea-stripped ROS membranes were treated with alkaline phosphatase (0.01 unit) for 30 min at 30 °C to ensure that there was no residual phosphate on rhodopsin and then were washed in 20 mM Hepes buffer to remove phosphatase. ROS membranes were subsequently phosphorylated by incubation with PKC-α (125 nM), 5 mM $MgCl_2$ and 100 μM ATP, as described, for 60 min [17]. Reactions were quenched with SDS/PAGE sample buffer and samples were analysed in duplicate on 10 % (w/v) polyacrylamide gels. One set of gels was stained with Coomassie Blue to detect protein, rhodopsin bands were excised, and ^{32}P incorporation into rhodopsin was quantified by liquid scintillation counting. Samples from the second set of gels were transferred on to PVDF for Western blot analysis. Blots were probed with 1 : 1000 dilutions of monoclonal 1D4 and polyclonal α-P334 and α-P338 antibodies.

In vivo time course of rhodopsin phosphorylation

Albino (Balb/c) mice were raised with a light/dark cycle of 12 h : 12 h until the age of 10 weeks. Mice were dark-adapted overnight before light exposure. The experiment was initiated by illuminating the mice with 100 lux white light (small light box). At appropriate time points, mice were killed and both retinas were harvested by dissection. Retinas were immediately flash frozen, then resuspended and homogenized in SDS/PAGE sample buffer. Two retinas were analysed for each time point. Three separate gels were run: two for Western blot analyses (0.2 retina per lane), with each of the two phosphospecific antibodies, and one for Western blot analysis (0.02 retinas per lane), with an antibody that does not discriminate between phosphorylation states of rhodopsin, 1D4. Antibody staining was detected by chemiluminescence and was quantified by CCD (charge-coupled device) camera using a GeneGnome bioimaging system (Syngene, Frederick, MD, U.S.A.).

Rhodopsin-kinase-knockout mice

Mice, aged approx. 6 months, were generated in a pigmented (C57/B6) background by Dr Jason Chen (Departments of Ophthalmology and Human Genetics, University of Utah, Salt Lake City, UT, U.S.A.) as described in [22] and were exposed to 1000 lux white light. Pigmented rhodopsin-kinase-knockout mice, wild-type pigmented litter-mates and albino controls were illuminated together for specified times. Total opsin was detected using α-opsin polyclonal antibodies.

In situ retina experiments

Retinas from albino mice were dissected under dim red light, at which point retinas from each mouse were separated into two tubes containing 1 ml of DMEM. Retinas were allowed to equilibrate for 15 min before the addition of 1 μM PMA to one retina and DMSO to the other retina from the same mouse. The retinas were incubated with PMA or DMSO for 15 min before illumination with 325 lux white light. After 15 min of constant light, the retinas were removed from the solution and were flash frozen. Retinas were solubilized in 1 ml of SDS/PAGE sample buffer and one-tenth of the sample was analysed with each phosphospecific antibody, and one-hundredth was analysed using the total opsin antibody, 1D4.

Immunoelectron microscopy

After exposure to light (see the '*In vivo* time course of rhodopsin phosphorylation' section above), eyes were quickly removed from the mice and immersed in 1 % (w/v) glutaraldehyde and 2 % (w/v) paraformaldehyde in 0.1 M phosphate buffer (pH 7.4). The eyes were then processed as described in [23]. Anterior segments were immediately dissected away while in fixative to yield eyecups. After 2 h at room temperature (25 °C), the eyecups were then dissected into small pieces. The retinal pieces were dehydrated through an ethanol series up to 90 %, infiltrated in a 1 : 1 mixture of LR White resin (Electron Microscopy Sciences, Fort Washington, PA, U.S.A.) and 90 % ethanol for 1 h, and then infiltrated overnight in pure LR White at 4 °C. They were

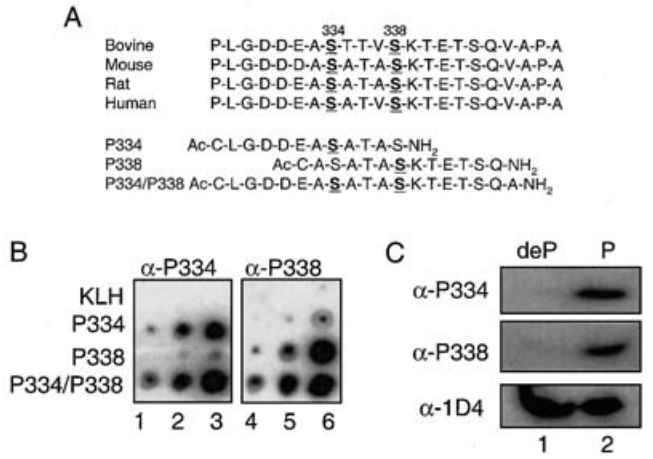

Figure 1 Phosphospecific antibodies

(**A**) Sequence alignment of bovine [27], mouse [28], rat [29] and human [30] rhodopsin, showing the positions of both major *in vivo* phosphorylation sites, Ser^{334} and Ser^{338}. The sequence of each phosphopeptide synthesized for antibody generation is shown at the bottom of the alignment; underlined S represents phosphoserine at position 334 or 338. (**B**) Dot blot showing reactivity of affinity-purified phosphospecific antibody α-P334 or α-P338 with 1 ng (lanes 1 and 4), 10 ng (lanes 2 and 5) or 100 ng (lanes 3 and 6) of KLH alone, the immunizing peptide KLH-coupled P334, the immunizing peptide KLH-coupled P338, or the doubly-phosphorylated KLH-coupled P334/P338 peptide (see the Experimental section for the sequences). (**C**) Western blot of purified phosphorylated bovine rhodopsin (lane 2) or that treated with alkaline phosphatase to ensure quantitative dephosphorylation (lane 1). Blots were probed with 1D4 monoclonal antibody to detect total rhodopsin or with phosphospecific antibodies α-P334 and α-P338.

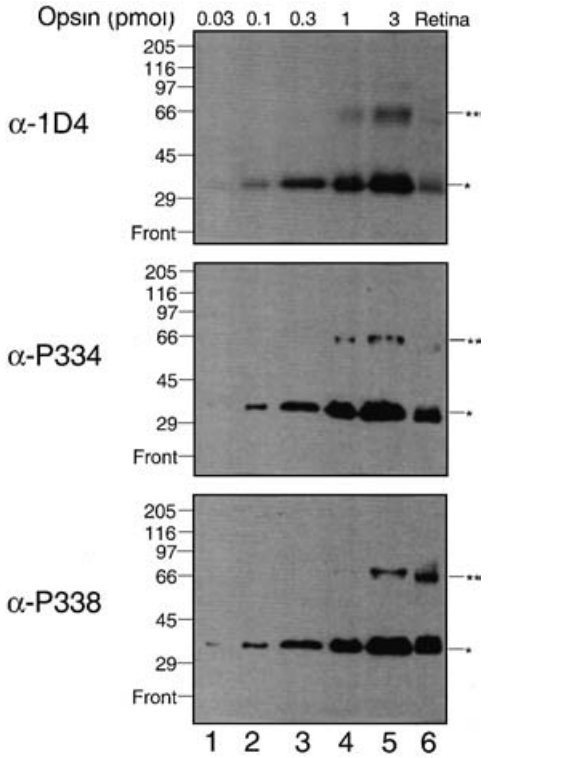

Figure 2 Quantification of phosphospecific antibody staining

Rhodopsin from urea-stripped membranes was phosphorylated *in vitro* by PKC-α to a stoichiometry of 0.15 mol of phosphate at Ser^{334} and 0.15 mol of phosphate at Ser^{338}. Triplicate Western blots with 0.03–3 pmol of opsin (lanes 1–5) were probed with 1D4, α-P334 and α-P338 antibodies to generate a standard curve. Both phosphospecific antibody blots were exposed for the same length of time. Lane 6 represents a retinal sample from mice exposed to illumination and corresponds to the 30 min *in vivo* sample seen in Figure 3. The single asterisk refers to the rhodopsin monomer and the double asterisk refers to the rhodopsin dimer.

embedded in the fresh resin and polymerized at 60 °C for 24 h. Ultrathin sections (60–70 nm) were collected on Formvar-coated nickel grids. Sections were first etched with saturated sodium periodate (Sigma), then blocked with 4 % (w/v) BSA in PBS for 30 min. The primary incubation was carried out overnight at 4 °C with affinity-purified α-P334 and α-P338 antibodies (1 : 800 dilution) in PBS containing 1 % (w/v) BSA. The sections were rinsed with PBS, and were then incubated with goat anti-rabbit IgG conjugated to 10 nm diameter gold particles (Amersham Biosciences) at a dilution of 1 : 30 in PBS with 1 % (w/v) BSA for 1 h. Sections were post-fixed in 2 % (w/v) glutaraldehyde for 20 min, washed in distilled water and stained with 5 % (w/v) uranyl acetate for 5 min before observation. They were then observed in a JEOL (Model 1200-EX) transmission electron microscope. Electron microscopy (EM) negatives were scanned in an Agfa Duoscan T2500 scanner.

RESULTS AND DISCUSSION

Generation and characterization of phosphospecific antibodies

To examine the spatial and temporal phosphorylation of two major *in vivo* rhodopsin phosphorylation sites in live animals, we generated phosphospecific antibodies against Ser^{334} and Ser^{338} on the C-terminal tail of rhodopsin (Figure 1A). Two phosphopeptides, P334 and P338, were chemically synthesized and used to generate α-P334 and α-P338 antibodies (see the Experimental section). Both antibodies were tested for phosphospecificity by probing KLH-coupled phosphopeptides or KLH alone immobilized on nitrocellulose with affinity-purified antibodies. Figure 1(B) shows that each antibody was specific for the phosphorylated residue it was generated against: α-P334 exclusively labelled the P334 peptide, and α-P338 exclusively labelled the P338 peptide. Importantly, phosphorylation at a second position did not affect the affinity of the antibody for the first site: Figure 1(B) shows that the α-P334 antibody bound the peptide phosphorylated at Ser^{334} and the peptide phosphorylated at both Ser^{334} and Ser^{338} equally well. Similarly, the α-P338 antibody recognized the peptide phosphorylated at Ser^{338} and the peptide phosphorylated at both Ser^{338} and Ser^{334} with comparable affinity. The phosphospecific antibodies were further characterized on Western blots using full-length rhodopsin: each antibody effectively labelled phosphorylated bovine rhodopsin (Figure 1C, lane 2), but not unphosphorylated rhodopsin (Figure 1C, lane 1). Thus each antibody was specific for phosphorylated rhodopsin at the relevant phosphorylation site and labelled the site against which it was directed, independently of phosphorylation at other sites.

We next addressed the sensitivity of the phosphospecific antibodies towards various concentrations of rhodopsin phosphorylated to a known stoichiometry (Figure 2). Rhodopsin was phosphorylated *in vitro* with pure PKC-α to a stoichiometry of 0.4 mol of phosphate per mol of rhodopsin. We have shown previously that, under the conditions of these phosphorylation assays, Ser^{334} and Ser^{338} each incorporate approx. 35 % of the total phosphate [17]. Thus, in the experiment in Figure 2, each site was phosphorylated to a stoichiometry of 0.15 mol of phosphate per mol of rhodopsin. Triplicate blots were analysed with either antibody 1D4 to probe for total opsin or the phosphospecific antibodies α-P334 and α-P338. Opsin migrated primarily as a monomer (Figure 2, single asterisk), with some dimer apparent

at the highest concentrations (Figure 2, double asterisks). Antibody 1D4 detected the lowest concentration of rhodopsin tested: 0.03 pmol (Figure 2, lane 1). Both α-P334 and α-P338 detected the second lowest concentration of phosphorylated opsin: 0.1 pmol (Figure 2, lane 2). This corresponds to a detection limit for each phosphospecific antibody of 0.02 pmol of phosphate per site. Thus both phosphospecific antibodies have similar affinities for phosphorylated sequences and are highly sensitive, with detection down to 0.02 pmol of phosphate. This analysis also included a sample of retina from a live mouse exposed to illumination (Figure 2, lane 6). Quantification of the intensities of the signals in the blots revealed that 0.09 pmol of opsin had been analysed and that it was phosphorylated to a stoichiometry of 0.3 pmol of phosphate on Ser^{334} and 0.2 pmol of phosphate on Ser^{338}.

Temporal differences in phosphorylation of Ser^{334} and Ser^{338} in mice exposed to light

We first took advantage of the phosphospecific antibodies to explore the time-dependence of phosphorylation at Ser^{334} and Ser^{338} in mice exposed to constant illumination. Albino mice were dark-adapted overnight to ensure quantitative dephosphorylation of rhodopsin and were then exposed to constant illumination (approx. 100 lux). Mice were killed immediately before illumination or after 1, 10, 30 or 60 min illumination. Lane 1 of Figure 3(A) shows that rhodopsin from dark-adapted animals was not labelled by either phosphospecific antibody, but was labelled by a monoclonal antibody to rhodopsin that does not discriminate between phosphorylation states, 1D4. Following 1 min of illumination, weak, but readily detectable, labelling by α-P338 antibody was observed, whereas barely detectable labelling was observed using α-P334 antibody (Figure 3A, lane 2). The labelling by α-P338 antibody peaked at 10 min (Figure 3A, lane 3), when the signal had increased dramatically to > 1000-fold that of the background. The signal then decreased with similar kinetics to its appearance, with approx. 10 % of the maximal signal observed following 60 min of illumination. In contrast with the rapid and transient labelling by α-P338 antibody, the labelling by α-P334 antibody continued to increase slowly through 60 min of illumination (Figure 3A, lane 5). The stoichiometry of phosphorylation at each site was determined using the standard curve in Figure 2. The kinetics of phosphorylation at each site are plotted in Figure 3(B), where the stoichiometry is plotted as a function of illumination time. These results reveal that (i) Ser^{338} is phosphorylated much more rapidly than Ser^{334}, and (ii) phosphate on Ser^{338} is considerably more labile than phosphate on Ser^{334}. Using MS analysis of thousands of retinas, Palczewski and coworkers [24] obtained similar results, showing that constant illumination resulted in rapid phosphorylation followed by dephosphorylation of Ser^{338}, as well as slower, but sustained, phosphorylation of Ser^{334}.

Spatial differences in phosphorylation of Ser^{334} and Ser^{338}

The generation of phosphospecific antibodies allowed us the unique opportunity to explore the spatial distribution of rhodopsin phosphorylated at each site using EM. Retinas from mice exposed to the same illumination conditions as those for the experiment shown in Figure 3 were isolated and fixed for use in EM. Figure 4 shows that, following 5 min illumination, Ser^{338} staining occurred over the entire length of the ROS. In contrast, staining by α-P334 antibody was concentrated in the proximal end of the ROS. Following 60 min of illumination, the entire ROS was evenly phosphorylated at Ser^{334} and Ser^{338}, as judged by uniform

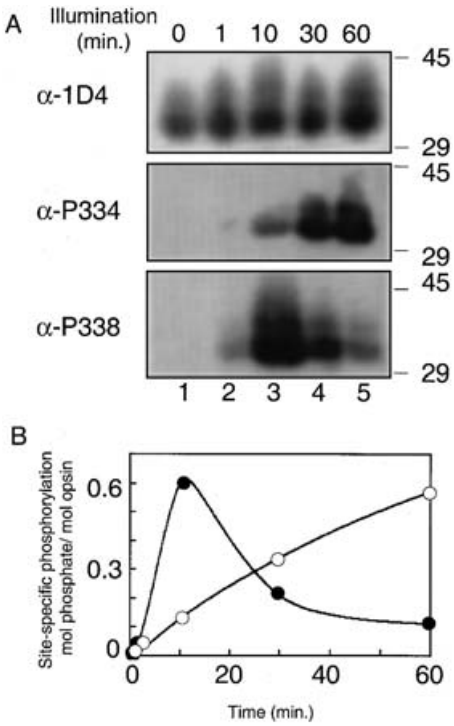

Figure 3 Time course of phosphorylation at Ser^{334} or Ser^{338} in mice exposed to light

(**A**) Albino mice were exposed to constant illumination (approx. 100 lux) to induce phosphorylation of rhodopsin. Retinas were dissected and quenched at the indicated times, then subjected to SDS/PAGE and Western blot analysis, as described in the Experimental section. Two retinas were quenched at each time point and one tenth (1D4) or one hundredth (α-P334 and α-P338) of the total sample was loaded per lane. Blots were probed for total opsin with the monoclonal 1D4 antibody (1D4), or with affinity-purified phosphospecific antibodies, α-P334 or α-P338. (**B**) The data from the Western blots shown in (**A**) was quantified by a CCD (charge-coupled-device) camera using a GeneGnome bioimaging system. To analyse the amount of phospho-Ser^{338} (closed circles) or phospho-Ser^{334} (open circles), results were normalized to total opsin; this phosphorylation stoichiometry is plotted as a function of illumination time. Results are representative of three independent experiments.

labelling with these two phosphospecific antibodies (results not shown). In addition, the overall level of labelling by α-P338 antibody was considerably reduced at 60 min compared with 5 min, consistent with the biochemical analysis from Figure 3 that showed that most of the rhodopsin was dephosphorylated at Ser^{338} following 60 min of illumination. Retinas from dark-adapted mice were not significantly labelled by either antibody (results not shown). These results indicate a spatial distribution of rhodopsin phosphorylation at Ser^{334} and Ser^{338} that has not previously been reported.

One possible explanation for a gradient of phosphorylation could be the direction of light input. Incoming light presumably strikes the proximal region of ROSs initially, and, over time, proceeds distally. However, the observed gradient of phosphorylation at Ser^{334} is present following 5 min of constant illumination, well after light has activated rhodopsin at the distal tip of the ROS, as demonstrated by P338 staining. As a result, it is unlikely that the gradient of Ser^{334} phosphorylation results directly from the direction of light input. An alternative possibility is that phosphorylation of Ser^{338} (or possibly Ser^{343} [19]) is required to 'prime' rhodopsin for subsequent phosphorylation at Ser^{334}. This priming step would probably also involve the dephosphorylation of Ser^{338}, because phosphorylation of Ser^{334} becomes significant only after Ser^{338} phosphorylation has peaked (see Figure 3B).

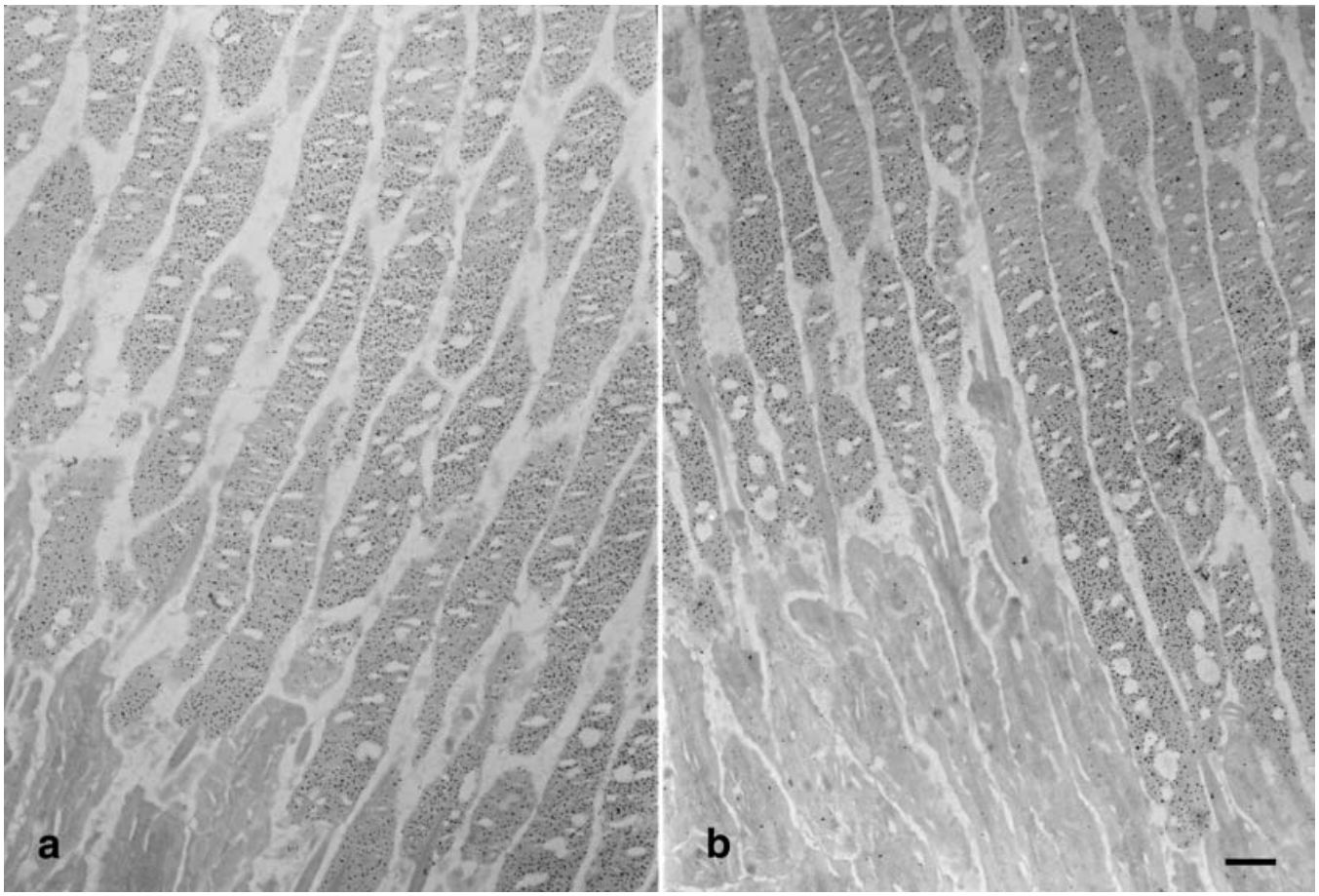

Figure 4 Spatial phosphorylation of rhodopsin within the rod photoreceptor

EM immunogold labelling of phosphorylated rhodopsin in ROSs with affinity-purified α-P338 (**A**) and α-P334 (**B**) antibodies. Retinas were obtained from mice after 5 min of light exposure. Sections from the same retina are shown in (**A**) and (**B**). The α-P338 antibody labels the ROS evenly (even the very distal region, which is not shown, was labelled at the same intensity). In contrast, labelling with the α-P334 antibody is concentrated in the proximal region. Both panels are at the same magnification, with the scale bar representing 1 μm.

RK is required for phosphorylation of Ser^{334} and Ser^{338}

The delayed temporal and spatial distribution of Ser^{334} phosphorylation compared with Ser^{338} phosphorylation led us to explore the role of a second kinase in regulating rhodopsin phosphorylation *in vivo*. First, we asked whether or not phosphorylation by RK was necessary for phosphorylation at Ser^{334}, the candidate site for a second kinase, using RK knock-out mice. RK$^{-/-}$ pigmented mice, as well as their wild-type control litter-mates, were exposed to light for increasing amounts of time. Since these animals were bred into a pigmented background, we increased the light intensity 10-fold to compensate for less efficient absorption of light by rhodopsin. Albino mice were included to assess whether these lighting conditions simulated the previous time course.

The upper panel in Figure 5(A) shows the total opsin in retinal samples from pigmented RK knockout mice (Figure 5A, lanes 1–3), pigmented wild-type litter-mates (Figure 5A, lanes 4–6), and albino wild-type mice (Figure 5A, lanes 7–9). Slightly less opsin was detected in the RK$^{-/-}$ mice as they were raised with a light/dark cycle of 12 h : 12 h. This lowered amount of opsin probably arises because the ROSs from RK$^{-/-}$ animals undergo light-induced apoptosis and are thus shorter than the ROSs of wild-type mice [22]. Comparison of data from wild-type pigmented (Figure 5A, lanes 4–6) and albino (Figure 5A, lanes 7–9) mice revealed similar kinetics of phosphorylation of Ser^{334} and similar stoichiometry (i.e. the ratio of labelling by α-P334 antibody to total opsin was the same in the albino and pigmented mice). The kinetics of labelling by α-P338 antibody were also similar for the two wild-type mice strains, but differed from the labelling observed for albino mice at lower light levels in that the phosphorylation was sustained. This sustained phosphorylation at both sites could arise from the increased light intensity, which presumably pushes the phosphorylated/dephosphorylated equilibrium towards the phosphorylated state. Curiously, the labelling by α-P338 antibody was markedly reduced (approx. 3-fold) in the pigmented mice relative to the albino mice. Assuming that the only difference between these wild-type mice strains is a lack of pigment in the albino mice, then this difference can be accounted for by the increased light sensitivity of the albino mice. The finding that pigmentation affects phosphorylation of Ser^{338}, but not Ser^{334}, underscores the possibility that the phosphorylation of each site is under the control of two mechanisms, and suggests further that phosphorylation of Ser^{338} has greater light-dependence than that of Ser^{334}.

Phosphorylation of both Ser^{334} and Ser^{338} was not observed in RK$^{-/-}$ mice (Figure 5A, lanes 1–3), even following 4 h exposure to constant illumination. The faint signal at the appropriate molecular mass for rhodopsin in the RK$^{-/-}$ mice results from non-specific labelling of a non-rhodopsin protein, since this band

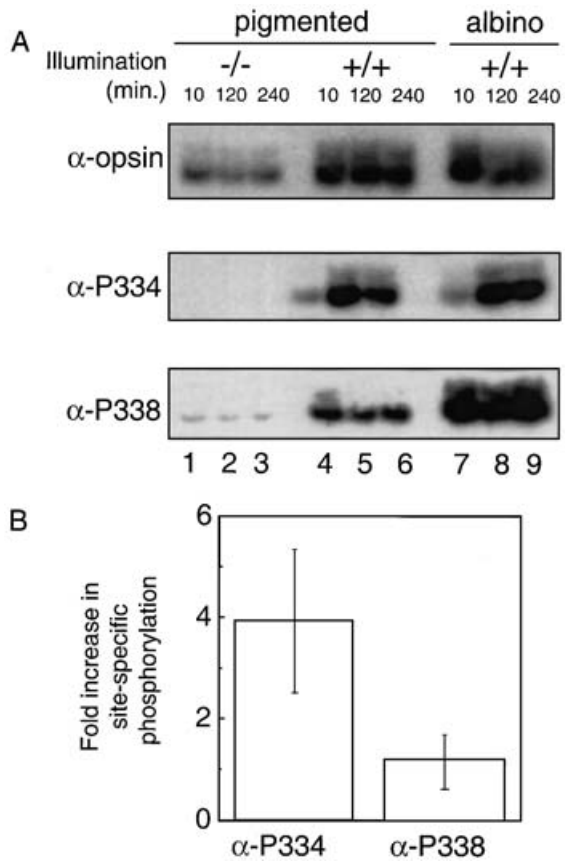

Figure 5 Rhodopsin phosphorylation following genetic or pharmacological manipulation of kinases

(**A**) The light-dependent phosphorylation of rhodopsin was examined in RK$^{-/-}$ pigmented mice (−/−; lanes 1–3), wild-type littermates (+/+ pigmented; lanes 4–6) and wild-type albino mice (+/+ albino; lanes 7–9). Mice were dark-adapted overnight and then exposed to constant illumination (approx. 1000 lux). Two retinas were quenched at each time point and one-hundredth (α-opsin antibody) or one-tenth (α-P334 and α-P338 antibodies) of the total sample was loaded per lane. Blots were probed with the polyclonal α-opsin antibody to probe for total opsin (upper panel), α-P334 antibody to probe for phospho-Ser^{334} (middle panel) or α-P338 antibody to probe for phospho-Ser^{338} (lower panel). Results are representative of two independent experiments. (**B**) Retinas from albino mice were removed and incubated in DMEM under dim red light and then treated with 1 μM PMA or solvent (DMSO) for 15 min at room temperature. The retinas were then illuminated (approx. 325 lux) for 15 min, conditions established to promote robust phosphorylation of both Ser^{334} and Ser^{338} (results not shown). Phosphorylation at each position was analysed by Western blot, and relative amounts of phosphorylation were quantified by CCD (charge-coupled-device) camera using a GeneGnome bioimaging system. Results are means $\pm$ S.E.M. ($n = 17$).

remains following boiling of these samples to quantitatively abolish monomeric rhodopsin on SDS/PAGE (results not shown). This lack of phosphorylation at both sites is consistent with MS studies of RK$^{-/-}$ mice showing > 10-fold reduction in total light-dependent rhodopsin phosphorylation [22].

Phosphorylation of Ser^{334} is increased following the activation of PKC

The RK$^{-/-}$ studies suggest that RK is required for rhodopsin phosphorylation at both Ser^{334} and Ser^{338}. Electrophysiological studies also support the requirement of RK for normal deactivation kinetics [25]. This necessity for RK could arise because of an ordered phosphorylation mechanism in which Ser^{338} must be phosphorylated first to allow a second kinase to phosphorylate the more slowly phosphorylated site, Ser^{334}. Since PKC activity modulates the phosphorylation state of rhodopsin *in vivo*, we explored the effects of PMA on the light-dependent phosphorylation of Ser^{334} and Ser^{338}. Retinas from albino mice were dissected and incubated with or without 1 μM PMA and were then exposed to constant illumination for 15 min. As previously shown, this is a condition which causes an increase in the light-dependent phosphorylation of rhodopsin using ^{32}P as a phosphorylation indicator [25]. Figure 5(B) demonstrates that PMA treatment caused a 4-fold increase in the phosphorylation of Ser^{334} relative to control retinas treated with DMSO. In contrast, PMA treatment had no significant increase on the phosphorylation of Ser^{338}. We have previously shown that phorbol ester treatment of retinas does not affect RK activity [14]. The time course in Figure 3(B) reveals that rhodopsin phosphorylation on Ser^{338} peaked at the time point used in the PMA study, whereas only modest phosphorylation of Ser^{334} had occurred.

The finding that PMA selectively increases the phosphorylation of Ser^{334}, a site that is an effective *in vitro* phosphorylation site of PKC, but not RK, suggests that this kinase may directly phosphorylate Ser^{334}. Although it is possible that RK is the kinase responsible for the phosphorylation of Ser^{334}, this seems unlikely given that the primary RK site, Ser^{338}, is not sensitive to PMA. The lack of phosphorylation at Ser^{334} in RK$^{-/-}$ mice indicates that initial phosphorylation by RK, presumably at Ser^{338}, is required to allow phosphorylation by PKC. Note, however, it is unlikely that rhodopsin that is phosphorylated at Ser^{338} is the substrate of PKC, since phosphorylation of Ser^{334} becomes significant well after dephosphorylation of Ser^{338}. Thus it is more likely that, following dephosphorylation of Ser^{338}, the conformation or macromolecular interactions of rhodopsin are altered in a manner to allow PKC recognition. Such alterations could arise from isomerization of neighbouring proline residues by prolyl isomerases that may be phosphorylation-specific [26]. Alternatively, the second-messenger pathway activating PKC could depend on the activity of RK.

CONCLUSIONS

Previous studies have clearly established the requirement of phosphorylation at Ser^{334} and Ser^{338} in controlling the physiological function of rhodopsin [22,25]. In the present study, we take advantage of phosphospecific antibodies to show that the phosphorylation of these sites is under the co-ordinated regulation of two mechanisms. There is an initial priming phosphorylation catalysed by RK at Ser^{338} and, based on the study of Hurley and co-workers [19], probably Ser^{343}. This species of rhodopsin is rapidly dephosphorylated, an event which allows for the phosphorylation of Ser^{334}. The second, but not first, phosphorylation mechanism is controlled by PKC as phorbol esters promote the phosphorylation of Ser^{334}, but not Ser^{338}. Our finding that PKC activation selectively affects the phosphorylation of Ser^{334} is consistent with this residue being a major *in vitro* site for PKC [17]. The use of phosphospecific antibodies, coupled with genetic and pharmacological manipulation of kinases, has allowed, for the first time, insight into the temporal and spatial regulation of rhodopsin phosphorylation. This significantly underscores the key role of a priming kinase, RK, and a secondary kinase, PKC, in rhodopsin function.

We thank Mel Simon and Jason Chen for generously providing RK$^{-/-}$ mice, Ulrike Katerkamp for help with the mouse experiments and Robert Molday for the generously supplying the monoclonal antibody, 1D4. This work was supported by NEI Grants EY08820 and EY12598 and NIH training grant 5T32DK07233 (to R. A. A.).

REFERENCES

1 Khorana, H. G. (1992) Rhodopsin, photoreceptor of the rod cell. J. Biol. Chem. **267**, 1–4
2 Hargrave, P. A. and McDowell, J. H. (1992) Rhodopsin and phototransduction: a model system for G protein-linked receptors. FASEB J. **6**, 2323–2331
3 Okada, T. and Palczewski, K. (2001) Crystal structure of rhodopsin: implications for vision and beyond. Curr. Opin. Struct. Biol. **11**, 420–426
4 Kühn, H. (1978) Light-regulated binding of rhodopsin kinase and other proteins to cattle photoreceptor membranes. Biochemistry **17**, 4389–4395
5 Wilden, U. and Kühn, H. (1982) Light-dependent phosphorylation of rhodopsin: number of phosphorylation sites. Biochemistry **21**, 3014–3022
6 Palczewski, K., McDowell, J. H. and Hargrave, P. A. (1988) Purification and characterization of rhodopsin kinase. J. Biol. Chem. **263**, 14067–14073
7 Palczewski, K., Buczylko, J., Kaplan, M. W., Polans, A. S. and Crabb, J. W. (1991) Mechanism of rhodopsin kinase activation. J. Biol. Chem. **266**, 12949–12955
8 Lorenz, W., Inglese, J., Palczewski, K., Onorato, J. J., Caron, M. G. and Lefkowitz, R. J. (1991) The receptor kinase family: primary structure of rhodopsin kinase reveals similarities to the β-adrenergic receptor kinase. Proc. Natl. Acad. Sci. U.S.A. **88**, 8715–8719
9 Pullen, N. and Akhtar, M. (1994) Rhodopsin kinase: studies on the sequence of and the recognition motif for multiphosphorylations. Biochemistry **33**, 14536–14542
10 Ohguro, H., Palczewski, K., Ericsson, L. H., Walsh, K. A. and Johnson, R. S. (1993) Sequential phosphorylation of rhodopsin at multiple sites. Biochemistry **32**, 5718–5724
11 McDowell, J. H., Nawrocki, J. P. and Hargrave, P. A. (1993) Phosphorylation sites in bovine rhodopsin. Biochemistry **32**, 4968–4974
12 Newton, A. C. and Williams, D. S. (1993) Does protein kinase C play a role in rhodopsin desensitization? Trends Biochem. Sci. **18**, 275–277
13 Newton, A. C. and Williams, D. S. (1991) Involvement of protein kinase C in the phosphorylation of rhodopsin. J. Biol. Chem. **266**, 17725–17728
14 Newton, A. C. and Williams, D. S. (1993) Rhodopsin is the major *in situ* substrate of protein kinase C in rod outer segments of photoreceptors. J. Biol. Chem. **268**, 18181–18186
15 Udovichenko, I. P., Newton, A. C. and Williams, D. S. (1997) Contribution of protein kinase C to the phosphorylation of rhodopsin in intact retinas. J. Biol. Chem. **272**, 7952–7959
16 Greene, N. M., Williams, D. S. and Newton, A. C. (1995) Kinetics and localization of the phosphorylation of rhodopsin by protein kinase C. J. Biol. Chem. **270**, 6710–6717
17 Greene, N. M., Williams, D. S. and Newton, A. C. (1997) Identification of protein kinase C phosphorylation sites on bovine rhodopsin. J. Biol. Chem. **272**, 10341–10344
18 Ohguro, H., Johnson, R. S., Ericsson, L. E., Walsh, K. A. and Palczewski, K. (1994) Control of rhodopsin multiple phosphorylation. Biochemistry **33**, 1023–1028
19 Kennedy, M. J., Lee, K. A., Niemi, G. A., Craven, K. B., Garwin, G. G., Saari, J. C. and Hurley, J. B. (2001) Multiple phosphorylation of rhodopsin and the *in vivo* chemistry underlying rod photoreceptor dark adaptation. Neuron **31**, 87–101
20 Mendez, A., Burns, M. E., Roca, A., Lem, J., Wu, L. W., Simon, M. I., Baylor, D. A. and Chen, J. (2000) Rapid and reproducible deactivation of rhodopsin requires multiple phosphorylation sites. Neuron **28**, 153–164
21 Papermaster, D. S. and Dreyer, W. J. (1974) Rhodopsin content in the outer segment membranes of bovine and frog retinal rods. Biochemistry **13**, 2438–2444
22 Chen, C. K., Burns, M. E., Spencer, M., Niemi, G. A., Chen, J., Hurley, J. B., Baylor, D. A. and Simon, M. I. (1999) Abnormal photoresponses and light-induced apoptosis in rods lacking rhodopsin kinase. Proc. Natl. Acad. Sci. U.S.A. **96**, 3718–3722
23 Liu, X., Udovichenko, I. P., Brown, S. D., Steel, K. P. and Williams, D. S. (1999) Myosin VIIa participates in opsin transport through the photoreceptor cilium. J. Neurosci. **19**, 6267–6274
24 Ohguro, H., Van Hooser, J. P., Milam, A. H. and Palczewski, K. (1995) Rhodopsin phosphorylation and dephosphorylation *in vivo*. J. Biol. Chem. **270**, 14259–14262
25 Lyubarsky, A. L., Chen, C., Simon, M. I. and Pugh, Jr, E. N. (2000) Mice lacking G-protein receptor kinase 1 have profoundly slowed recovery of cone-driven retinal responses. J. Neurosci. **20**, 2209–2217
26 Zhou, X. Z., Kops, O., Werner, A., Lu, P. J., Shen, M., Stoller, G., Kullertz, G., Stark, M., Fischer, G. and Lu, K. P. (2000) Pin1-dependent prolyl isomerization regulates dephosphorylation of Cdc25C and tau proteins. Mol. Cell **6**, 873–883
27 Nathans, J. and Hogness, D. S. (1983) Isolation, sequence analysis, and intron-exon arrangement of the gene encoding bovine rhodopsin. Cell **34**, 807–814
28 Baehr, W., Falk, J. D., Bugra, K., Triantafyllos, J. T. and McGinnis, J. F. (1988) Isolation and analysis of the mouse opsin gene. FEBS Lett. **238**, 253–256
29 Barnstable, C. J. and Morabito, M. A. (1994) Isolation and coding sequence of the rat rod opsin gene. J. Mol. Neurosci. **5**, 207–209
30 Nathans, J. and Hogness, D. S. (1984) Isolation and nucleotide sequence of the gene encoding human rhodopsin. Proc. Natl. Acad. Sci. U.S.A. **81**, 4851–4855

Received 13 March 2003/5 June 2003; accepted 16 June 2003
Published as BJ Immediate Publication 16 June 2003, DOI 10.1042/BJ20030408